8-1-1995

Gaussian, exponential, and power-law decay of time-dependent correlation functions in quantum spin chains

Joachim Stolze

Angela Nöppert

Gerhard Müller
University of Rhode Island, gmuller@uri.edu

Citation/Publisher Attribution

Joachim Stolze, Angela Nöppert, and Gerhard Müller. *Gaussian, exponential, and power-law decay of time-dependent correlation functions in quantum spin chains.* Phys. Rev. B 52 (1995), 4319-4326. Available at: http://dx.doi.org/10.1103/PhysRevB.52.4319

Gaussian, exponential, and power-law decay of time-dependent correlation functions in quantum spin chains

Gaussian, exponential, and power-law decay of time-dependent correlation functions in quantum spin chains

Joachim Stolze
Physikalisches Institut, Universität Bayreuth, 95440 Bayreuth, Germany
*and Institut für Physik, Universität Dortmund, 44221 Dortmund, Germany**

Angela Nöppert
Institut für Physik, Universität Dortmund, 44221 Dortmund, Germany

Gerhard Müller
Department of Physics, The University of Rhode Island, Kingston, Rhode Island 02881-0817
(Received 17 January 1995)

Dynamic spin correlation functions $\langle S_i^x(t)S_j^x\rangle$ for the one-dimensional $S=\frac{1}{2}$ XX model $H=-J\Sigma_i\{S_i^xS_{i+1}^x+S_i^yS_{i+1}^y\}$ are calculated exactly for finite open chains with up to $N=10\,000$ spins. Over a certain time range the results are free of finite-size effects and thus represent correlation functions of an infinite chain (bulk regime) or a semi-infinite chain (boundary regime). In the bulk regime, the long-time asymptotic decay as inferred by extrapolation is Gaussian at $T=\infty$, exponential at $0<T<\infty$, and power-law ($\sim t^{-1/2}$) at $T=0$, in agreement with exact results. In the boundary regime, a power-law decay is obtained at all temperatures; the characteristic exponent is universal at $T=0$ ($\sim t^{-1}$) and at $0<T<\infty$ ($\sim t^{-3/2}$), but is site dependent at $T=\infty$. In the high-temperature regime ($T/J\gg 1$) and in the low-temperature regime ($T/J\ll 1$), crossovers between different decay laws can be observed in $\langle S_i^x(t)S_j^x\rangle$. Additional crossovers are found between bulk-type and boundary-type decay for $i=j$ near the boundary, and between spacelike and timelike behavior for $i\neq j$.

I. INTRODUCTION

The long-time behavior of correlations for quantum many-body systems in general and for quantum spin systems in particular has been a notoriously difficult subject of theoretical research. Approximation schemes tend to have little reliability in this field. There exist very few exact results for nontrivial cases, and many of them exhibit nongeneric features for one reason or another. In classical many-body systems, long-time correlations can be investigated by means of computer simulations, but no practical quantum counterpart of that approach exists.

In some cases, useful conclusions on the long-time behavior can be drawn from a moment expansion via rigorous bounds, but the time intervals over which stringent bounds can be established are often too short for that purpose.[1–3] The continued-fraction analysis based on the same number of moments can be used to predict the exponent of a power-law infrared singularity in the frequency domain, but this approach tends to be insensitive to subtle changes in the long-time decay if it does not involve power laws.[4,5]

The one-dimensional (1D) $S=1/2$ XY model

$$H_{XY}=-\sum_{i=1}^{N-1}\{J_xS_i^xS_{i+1}^x+J_yS_i^yS_{i+1}^y+hS_i^z\} \quad (1.1)$$

is one of the very few many-body systems with nontrivial dynamics for which time-dependent correlation functions have been calculated exactly at zero[6–11] and nonzero[12–15] temperatures. This model is equivalent to a system of noninteracting lattice fermions.[16,17] The spin correlation function $\langle S_i^z(t)S_j^z\rangle$ is a simple fermion density correlation function, and the function $\langle S_i^x(t)S_j^x\rangle$ can be reduced to a determinant whose size increases linearly with the number of sites between i or j and the nearest boundary of the chain.

The focus of this study is on the dynamics of the spin x components for the special case $J_x=J_y$, $h=0$ of (1.1) — the XX model. For quite some time it has been known that the function $\langle S_i^x(t)S_i^x\rangle$ of the infinite system exhibits a Gaussian decay at $T=\infty$ (Refs. 12–14) and a power-law decay at $T=0$.[8,9] A more recent study states that the long-time asymptotic decay of the same correlation function is exponential at finite nonzero temperatures.[15] Numerical evidence for exponential decay was also found for $\langle S_i^x(t)S_i^x\rangle$ in the XXZ model at $T=\infty$.[5]

For a semi-infinite XX chain the available evidence indicates that the function $\langle S_i^x(t)S_i^x\rangle$ exhibits a power-law decay at all temperatures. Rigorous results exist for $T=\infty$,[4,18] and the result of a finite-chain study for $T=0$,[19] but no results for $0<T<\infty$ appear to have existed prior to this study.

The purpose of this paper is (i) to fill in the missing links on the question of long-time asymptotic behavior and (ii) to elucidate various kinds of crossovers between the different decay laws that can be found in the

autocorrelation and paircorrelation functions $\langle S_i^x(t)S_j^x\rangle$. The determinantal expressions for these functions have been known for a long time.[8] However, only with today's advanced computer technology can they be evaluated for systems large enough to yield data from which conclusions can be drawn with some confidence about the long-time asymptotics for infinite and semi-infinite chains at arbitrary temperatures.[20] In Sec. II we describe the method used for our analysis, in Sec. III we present our results for the infinite system, and in Sec. IV we discuss boundary effects.

II. FERMION REPRESENTATION

The Jordan-Wigner transformation[16,17]

$$S_i^z = a_i^\dagger a_i - \frac{1}{2}\,, \tag{2.1}$$

$$S_i^+ = (-1)^{\sum_{k=1}^{i-1} a_k^\dagger a_k} a_i^\dagger\,, \quad S_i^- = a_i (-1)^{\sum_{k=1}^{i-1} a_k^\dagger a_k}\,, \tag{2.2}$$

between the component and ladder operators S_i^z, $S_i^\pm = S_i^x \pm i S_i^y$ for an array of localized spins with $S = 1/2$ and the creation and annihilation operators $a_i^\dagger$, a_i of an array of fermions converts the Hamiltonian of an open-ended XX chain,

$$H_{XX} = -J \sum_{i=1}^{N-1} \left\{ S_i^x S_{i+1}^x + S_i^y S_{i+1}^y \right\}\,, \tag{2.3}$$

into a Hamiltonian of noninteracting fermions,

$$H_{XX} = -\frac{J}{2} \sum_{i=1}^{N-1} (a_i^\dagger a_{i+1} + a_{i+1}^\dagger a_i)\,. \tag{2.4}$$

The energies of the one-particle eigenstates are

$$\varepsilon_k = -J\cos k, \quad k = \frac{\nu\pi}{N+1}, \quad \nu = 1, \ldots, N\,. \tag{2.5}$$

The spin correlation functions $\langle S_i^z(t)S_j^z\rangle$ are then in essence density correlation functions for the band (2.5) of free fermions. Their characteristic t^{-1} long-time asymptotic behavior at zero and nonzero temperatures[6,7,11] is a consequence of the band-edge singularities in the one-particle density of state and (for $T = 0$) the singularity at $\omega = 0$ generated by the Fermi function. For the spins at the boundary of a semi-infinite chain, different power-law decays of $\langle S_i^z(t)S_j^z\rangle$ pertain to $T = 0$ ($\sim t^{-2}$ if both i and j are odd and $\sim t^{-3}$ otherwise) and $T > 0$ ($\sim t^{-3}$ for all i and j).[21] A boundary-to-bulk crossover can be observed for sites near the end of a semi-infinite chain at $T = \infty$.[4]

The correlation functions $\langle S_i^x(t)S_j^x\rangle$ have a much more complicated structure in the fermion representation. With the fermionic identity

$$(-1)^{a_k^\dagger a_k} = (a_k^\dagger + a_k)(a_k^\dagger - a_k) \tag{2.6}$$

applied to (2.2), this correlation function may be expressed in terms of the auxiliary operators $A_k = a_k^\dagger + a_k$ and $B_k = a_k^\dagger - a_k$ as follows:

$$\langle S_i^x(t)S_j^x\rangle = \frac{1}{4}\langle A_1(t)B_1(t)A_2(t)B_2(t)\cdots A_{i-1}(t)B_{i-1}(t)A_i(t)A_1B_1A_2B_2\cdots A_{j-1}B_{j-1}A_j\rangle\,. \tag{2.7}$$

This expectation value of a product of $2(i+j-1)$ fermion operators may be expanded via Wick's theorem in terms of more elementary expectation values. The result is most compactly expressed as a Pfaffian:[22]

$$4\langle S_i^x(t)S_j^x\rangle = \begin{vmatrix} \langle A_1(t)B_1(t)\rangle & \langle A_1(t)A_2(t)\rangle & \cdots & \langle A_1(t)A_1\rangle & \langle A_1(t)B_1\rangle & \cdots & \langle A_1(t)A_j\rangle \\ & \langle B_1(t)A_2(t)\rangle & \cdots & \langle B_1(t)A_1\rangle & \langle B_1(t)B_1\rangle & \cdots & \langle B_1(t)A_j\rangle \\ & & \cdots & \cdots & \cdots & \cdots & \cdots \\ & & & \cdots & \cdots & \cdots & \cdots \\ & & & & \cdots & \cdots & \cdots \\ & & & & & \cdots & \cdots \\ & & & & & & \langle B_{j-1}A_j\rangle \end{vmatrix}\,. \tag{2.8}$$

The square of the Pfaffian is equal to the determinant of the antisymmetric matrix with the elements of (2.8) above the diagonal. The matrix elements can be evaluated from the expressions[23]

$$\langle A_j(t)A_l\rangle = \frac{2}{N+1}\sum_k \sin kj \sin kl \left[\cos\varepsilon_k t - i\sin\varepsilon_k t \tanh\frac{\beta\varepsilon_k}{2}\right], \tag{2.9}$$

$$\langle A_j(t)B_l\rangle = \frac{2}{N+1}\sum_k \sin kj \sin kl \left[i\sin\varepsilon_k t - \cos\varepsilon_k t \tanh\frac{\beta\varepsilon_k}{2}\right], \tag{2.10}$$

and the relations

$$\langle B_j(t)B_l\rangle = -\langle A_j(t)A_l\rangle, \quad \langle B_j(t)A_l\rangle = -\langle A_j(t)B_l\rangle . \tag{2.11}$$

All elements (2.9) with odd $j-l$ and all elements (2.10) with even $j-l$ vanish. For $t=0$ the elements (2.9) are, in fact, zero for all $j \neq l$. All results for the correlation functions $\langle S_i^x(t)S_j^x\rangle$ of the XX model presented in the following have been derived via numerical evaluation of the determinant associated with (2.8) for systems with up to $N = 10\,000$ sites. The results are not subject to finite-size effects on the time intervals shown, except where this is explicitly stated.

III. BULK REGIME

The spin correlation function $\langle S_i^x(t)S_{i+n}^x\rangle$ of H_{XX} at $T=\infty$ is surprisingly simple: a pure Gaussian for $n=0$ and identically vanishing for $n \neq 0$:[12–14]

$$\langle S_i^x(t)S_{i+n}^x\rangle = \frac{1}{4}\delta_{n,0}\exp\left[-\frac{J^2t^2}{4}\right] \qquad (T=\infty). \tag{3.1}$$

No physical argument was ever furnished to explain this peculiar decay law. At $T=0$ that same spin correlation function exhibits a power-law decay, of which the leading term in an asymptotic expansion,[10]

$$\langle S_i^x(t)S_{i+n}^x\rangle = \frac{1}{4}\frac{\sqrt{2}A^2}{(n^2-J^2t^2)^{1/4}} \qquad (T=0), \tag{3.2}$$

with $A = 2^{1/12}\exp[3\zeta'(-1)] = 0.645\,002\,48...$, reflects the Luttinger liquid nature of the ground state of H_{XX}. Further terms of that expansion are known for general n and many more for $n=0$.[10,11]

Until recently it was not at all clear whether the Gaussian and power-type decay laws persist at any finite nonzero temperatures. Then Its *et al.*[15] established on a rigorous basis that $\langle S_i^x(t)S_{i+n}^x\rangle$ decays exponentially for $0 < T < \infty$, i.e., more slowly than (3.1), yet more rapidly than (3.2). From the solutions of the completely integrable discrete nonlinear Schrödinger model, which is related to H_{XX}, they were able to derive the following expression for the two-spin correlation function:

$$\langle S_i^x(t)S_{i+n}^x\rangle \propto \begin{cases} \exp f(n,0), & n/Jt > 1, \\ t^{4\nu^2}\exp f(n,t), & n/Jt < 1, \end{cases} \tag{3.3}$$

with

$$f(n,t) = \frac{1}{2\pi}\int_{-\pi}^{\pi} dp\,|n - Jt\sin p|\,\ln\left|\tanh\frac{J\cos p}{2T}\right|, \tag{3.4}$$

$$\nu = \frac{1}{2\pi}\ln\left|\tanh\frac{J\sqrt{1-(n/Jt)^2}}{2T}\right|, \tag{3.5}$$

valid in the spacelike ($n/Jt > 1$) or the timelike ($n/Jt < 1$) sectors of the long-time ($Jt \to \infty$) and/or long-distance ($n \to \infty$) asymptotic regime. The function $f(n,t)$ is negative and monotonically decreasing with increasing T; it diverges logarithmically at $T=\infty$, thus signaling the change in decay law.

In the high-temperature regime, the result (3.3) for the autocorrelation function ($n=0$) can be brought into the more explicit form:

$$\langle S_i^x(t)S_i^x\rangle \sim \exp\left[-\frac{2Jt}{\pi}\left(1+\ln\frac{2T}{J}\right)\right] \quad (1 \ll T/J < \infty). \tag{3.6}$$

What remains to be filled in for the bulk spin correlation functions $\langle S_i^x(t)S_{i+n}^x\rangle$ is to connect the exponential decay to the Gaussian decay ($n=0$) or the identically vanishing result ($n \neq 0$) in the high-temperature limit and to the power-law decay in the low-temperature limit. These connections are realized by crossovers between different decay laws at short and long times and can be investigated systematically in the data of finite systems. The salient features of the crossovers are described in Figs. 1 and 2 for autocorrelations ($n=0$) and in Fig. 3 for paircorrelations ($n \neq 0$).

A. Autocorrelations

The modulus-squared spin autocorrelation function $|\langle S_i^x(t)S_i^x\rangle|^2$ is plotted logarithmically in Fig. 1 for six values of T/J, all in the high-temperature regime (solid lines). The bulk character of these results for site $i=49$ of a chain with $N=100$ spins has been ascertained by comparison with the results of longer chains (with up to $N=1000$ spins). The (parabolic) dashed line represents the Gaussian (3.1) — the exact result for $T=\infty$.

We observe that the Gaussian behavior persists at finite T over some range of short times. That range shrinks

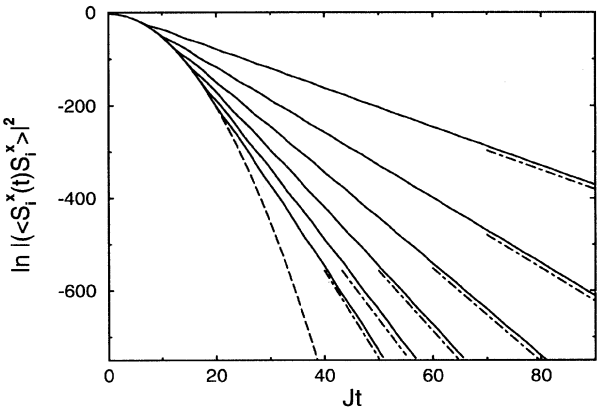

FIG. 1. Spin autocorrelation function $\langle S_i^x(t)S_i^x\rangle$ in the bulk regime of H_{XX} at high temperatures. Plotted is the logarithm of $|\langle S_i^x(t)S_i^x\rangle|^2$ evaluated at increments $Jdt = 0.4$ for site $i=49$ in an open chain of N=100 spins, for $2T/J = 10, 10^2, \ldots, 10^6$ (solid lines, top to bottom). The exact result (3.1) for $T=\infty$ is shown as dashed line. The slopes of the dot-dashed straight-line segments represent the decay rate of (3.6).

with decreasing temperature. From the common short-time parabolic shape the individual lines take off like a bundle of tangents, which represent the exponential character of the long-time decay. The crossover takes place quite suddenly.[24] The slight wiggles in the high-temperature data will turn into stronger oscillations in the low-temperature regime as we shall see. The observed decay rate in the exponential regime as represented by the slope of the tangent lines decreases monotonically as the temperature is lowered. It is well matched in each case by the slope of the adjacent dot-dashed line, which represents the decay rate

$$\frac{1}{\tau} = \frac{2J}{\pi}\left[1 + \ln\frac{2T}{J}\right] \qquad (T/J \gg 1) \qquad (3.7)$$

of the asymptotic result (3.6).

The solid lines in Fig. 2 show the same quantity as in Fig. 1 but now for three values of T/J in the low-temperature regime. Here the short-time Gaussian behavior has disappeared from the scene. The steepest curve corresponds to the highest temperature ($2T/J = 1.0$). The exponential nature of the decay (with mild oscillations superimposed) is now realized even at relatively short times. The average slope is perfectly consistent with the decay rate inferred from the asymptotic result (3.3), represented by the slope of the adjacent dot-dashed line.

At lower temperatures a crossover between exponential decay and power-law decay makes its appearance. The power-law behavior is first seen at short times. In the center curve of Fig. 2, the crossover takes place prior to $Jt = 20$. At longer times the exponential decay is still clearly visible, and the rate of decay agrees well with the asymptotic rate

$$\frac{1}{\tau} = T\left[\frac{\pi}{2} - \frac{4}{\pi}e^{-J/T} + \cdots\right] \qquad (T/J \ll 1) \qquad (3.8)$$

extracted from (3.3) (see adjacent dot-dashed line). The top curve in Fig. 2 represents the $T = 0$ result, which has been investigated in previous studies. The dashed line shows the asymptotic power law (3.2) for $n = 0$, which matches the data shown here extremely well (except for the oscillations).

The onset of finite-size effects at longer times is shown in the inset to Fig. 2 for two cases. The rebound of the $T = 0$ correlation function at $Jt \simeq 100$ can be interpreted as the echo from open ends of the ballistically propagating fermions. In the $T > 0$ case, the peak at $Jt \simeq 100$ is absent because of destructive interference. The first echo now occurs at $Jt \simeq 200$, the time it takes a pulse to move through the system twice. The speed of propagation which determines the echo time is given by the maximum fermion velocity $v = \max[d\epsilon_k/dk]$. For the dispersion (2.5) of H_{XX} we have $v = J$. In the presence of anisotropy as realized in the H_{XY} with $J_x \neq J_y$, ϵ_k acquires a gap, v decreases, and finite-size effects set in later.[25] These echo effects occur at all temperatures. They are easy to recognize in all data produced for this study.

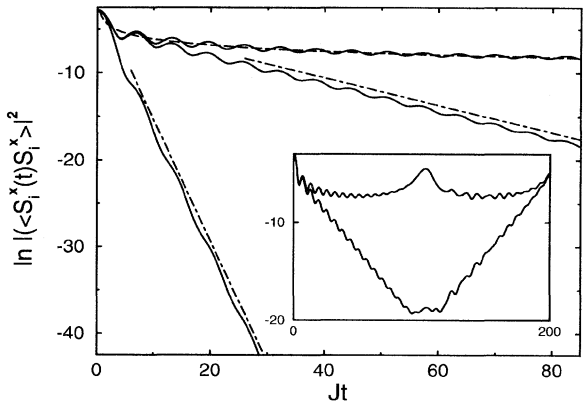

FIG. 2. Spin autocorrelation function $\langle S_i^x(t)S_i^x\rangle$ in the bulk regime of H_{XX} at low temperatures. Plotted is the logarithm of $|\langle S_i^x(t)S_i^x\rangle|^2$ evaluated at increments $Jdt = 0.4$ for site $i = 49$ in an open chain of $N = 100$ spins at $2T/J = 1.0, 0.1$ and for site $i = 249$ in a system of size $N = 500$ at $T = 0$ (solid lines, bottom to top). The dashed line represents (3.2). The slopes of the dot-dashed straight-line segments represent the decay rate inferred from the asymptotic expression (3.3). The inset shows the results at $2T/J = 0$ (upper curve) and 0.1 (lower curve) again over a longer time interval and (now in both cases) for $N = 100$ in order to illustrate the onset of finite-size effects in the form of echos due to ballistically propagating pulses reflected at the open ends of the chain.

B. Paircorrelations

In Fig. 3 we show a logarithmic plot of $|\langle S_i^x(t)S_{i+n}^x\rangle|^2$ for n=4, 9, 14, 19 at the intermediate temperature

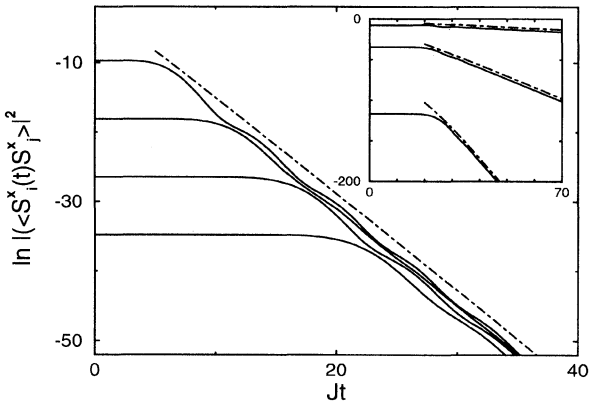

FIG. 3. Spin paircorrelation function $\langle S_i^x(t)S_j^x\rangle$ in the bulk regime of H_{XX} at $2T/J = 1$, for $j = 49$ and $i = 30$, 35, 40, and 45 (solid lines, top to bottom) in an open chain with $N = 100$ spins. Plotted is the logarithm of $|\langle S_i^x(t)S_j^x\rangle|^2$ evaluated at increments $Jdt = 0.4$ The inset shows the same function in the same representation, but here the sites are kept fixed ($i = 30, j = 49$) and the temperature is varied ($2T/J = 0.1, 1, 10$). The slopes of the dot-dashed straight-line segments represent the decay rate inferred from the asymptotic expression (3.3).

$2T/J = 1$. We observe that each function is almost perfectly constant up to a time $Jt_n \simeq n$, where it bends smoothly into exponential decay with superimposed oscillations. The decay time does not show any significant dependence on n. The inverse decay time predicted by (3.3) for the asymptotic regime of the uppermost curve is given by the slope of the dashed line and matches our data very well. A numerical analysis of (3.3) shows that the asymptotic decay time increases slightly with increasing n at fixed temperature. The linear variation with n of the intercepts at $Jt = 0$ in this logarithmic plot reflects the well-established exponential decay of the equal-time correlation function $\langle S_i^x S_{i+n}^x \rangle \sim \exp[-n/\xi(T)]$.

The inset to Fig. 3 shows again the curve $n = 19$ of the main plot along with curves for the same correlation function at different temperatures. Now the crossover between the spacelike and the timelike regimes occurs at one common value of Jt. In the timelike regime, the slope changes from one curve to the next, which reflects the T dependence of the decay time, while the variable intercept in the spacelike regime reflects the T dependence of the correlation length.

The correlation length $\xi(T)$ is known to diverge algebraically, $\sim 1/T$, at $T = 0$ and to vanish logarithmically, $\sim 1/\ln(T)$, at $T = \infty$.[26–28] We have noted in Sec. III A that the decay time $\tau(T)$ also goes to zero logarithmically at $T = \infty$ and exhibits the same power-law divergence at $T = 0$. Figure 4 shows both the inverse correlation length and the inverse decay time plotted versus temperature. In the XXZ model, the two quantities are expected to have more distinct temperature dependences. The numerical results of Ref. 5 indicate that $\tau(T)$ stays nonzero at $T = \infty$, whereas $\xi(T)$ is expected to vanish in that limit as it does in the XX model.

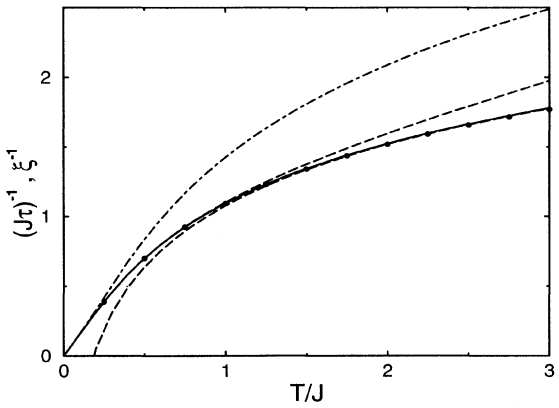

FIG. 4. Temperature dependence of the inverse decay time $1/\tau$ as derived from the asymptotic expression (3.3) (solid line) and from our numerical analysis of large but finite chains (circles). The numerical data were derived from an exponential fit to $|\langle S_i^x(t) S_i^x \rangle|^2$ for $i = 49$ in an open chain of $N = 100$ spins, evaluated for $20 \leq Jt \leq 60$ at increments $Jdt = 0.4$. The dashed lines represent the approximations (3.7) and (3.8) to (3.3) for high and low T, respectively. For comparison we also show (dot-dashed line) the temperature dependence of the inverse correlation length $1/\xi$ as given by (3.3). Data read off Fig. 2 of Ref. 28 coincide with the curve shown, as do data derived from our own numerical results for $\langle S_i^x S_j^x \rangle / \langle S_{i+1}^x S_j^x \rangle$ with $|i - j| = 10$ or 20 in an open chain of $N = 100$ spins.

IV. BOUNDARY EFFECTS

Here we investigate spin autocorrelation functions $\langle S_i^x(t) S_i^x \rangle$ of a semi-infinite chain for sites $i = 1, 2, \ldots$ beginning at the boundary. The actual calculations are performed for sites i near one end of a finite open chain (2.3) of N spins. However, none of the results presented are affected by the far end of the chain.

The long-time asymptotic decay of $\langle S_i^x(t) S_i^x \rangle$ in the boundary regime of a semi-infinite chain is different at zero, finite nonzero, and infinite temperatures. It is fastest at $T = \infty$ and slowest at $T = 0$, like in the bulk regime, but instead of seeing transitions from Gaussian to exponential to power-law decay, we now observe transitions between three types of power-law decay.

At infinite temperature, the power-law long-time asymptotic decay has the form

$$\langle S_i^x(t) S_i^x \rangle \sim t^{-3/2-(i-1)(i+1)} \qquad (T = \infty), \tag{4.1}$$

with a site-dependent exponent. This result was inferred from an exact calculation for sites $i = 1, 2, \ldots, 5$, and presumably holds for all sites of a semi-infinite chain.[4] The power-law decay at zero temperature as obtained from a perturbational treatment of the Pfaffian (2.8) is site independent,[19]

$$\langle S_i^x(t) S_i^x \rangle \sim t^{-1} \qquad (T = 0), \tag{4.2}$$

and different from the $t^{-1/2}$ decay in the bulk regime. Our numerical analysis of the same determinantal expression at finite nonzero temperatures strongly indicates that the long-time asymptotic decay is a power law with yet a different site-independent exponent:

$$\langle S_i^x(t) S_i^x \rangle \sim t^{-3/2} \qquad (0 < T < \infty). \tag{4.3}$$

An analytic calculation, which confirms this decay law, is presented in the Appendix. The five curves in Fig. 5 represent the quantity $|\langle S_i^x(t) S_i^x \rangle|^2$ for $i = 2$ at various temperatures in a log-log plot. The data are subject to strong oscillations, which makes it hard to distinguish the different decay laws in this graphical representation. Therefore we have smoothed the data at $Jt > 40$ as described in the caption. The three different slopes of the dashed lines represent the decay laws (4.1) – (4.3), i.e., $t^{-9/2}$ for $i = 2$ (bottom line), $t^{-3/2}$ (intermediate lines), and t^{-1} (top line).

The decay laws of $\langle S_i^x(t) S_i^x \rangle$ at a given temperature and for a given site on the semi-infinite chain may undergo one or several crossovers. Here we have to deal with bulk-to-boundary crossovers in addition to crossovers between different temperature regimes. We first look at the two types individually and then in combination.

At $T = \infty$ we observe a bulk-to-boundary crossover, i.e., a crossover from Gaussian decay (3.1) at short times

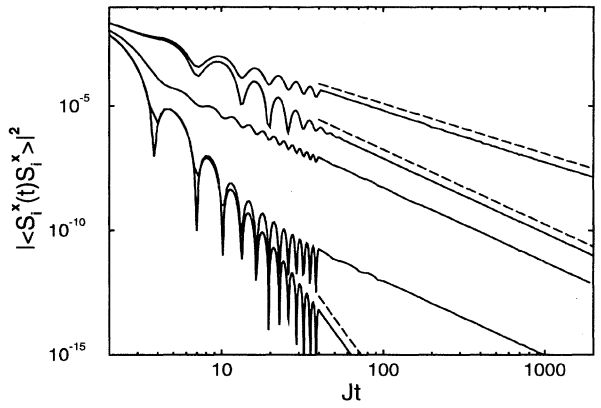

FIG. 5. Spin autocorrelation function $\langle S_i^x(t)S_i^x\rangle$ in the boundary regime of H_{XX} at $2T/J = 0, 0.1, 1, 10, \infty$ (solid lines, top to bottom). Shown is the quantity $|\langle S_i^x(t)S_i^x\rangle|^2$ evaluated at increments $Jdt = 0.4\,(Jt \leq 40)$, $Jdt = 1\,(40 \leq Jt \leq 100)$, and $Jdt = 10\,(100 \leq Jt \leq 2000)$ in a double logarithmic plot. The data pertain to the site $i = 2$ in an open chain of $N = 10\,000$ spins. At times $Jt > 40$ most of the data were smoothed by the following two-step procedure: (i) retain all local maxima of the data set; (ii) eliminate all local minima from the remaining data set. The $2T/J = 0.1$ data did not require smoothing. The dashed lines represent the power laws t^{-1} (top), $t^{-3/2}$ (center), and $t^{-9/2}$ (bottom).

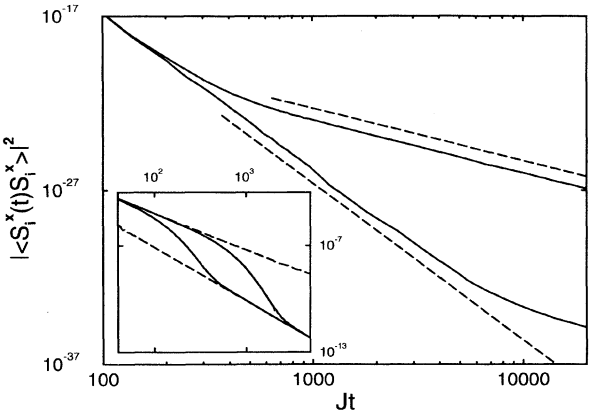

FIG. 7. The main plot shows smoothed data of the same quantity as in Fig. 5 at two very high temperatures ($2T/J = 10^3, 10^5$) and in the inset for two very low temperatures ($2T/J = 2 \times 10^{-3}, 10^{-2}$). The dashed lines in the main plot represent the power laws $t^{-3/2}$ (top) and $t^{-9/2}$ (bottom). The dashed lines in the inset represent data for temperatures $2T/J = 0, 0.1$ (i.e., the two uppermost solid lines of Fig. 5).

to power-law decay (4.1) at long times. This is illustrated in Fig. 6 for the sites $i = 2, \ldots, 11$ near the end of a semi-infinite chain. The time Jt_c marking the onset of the crossover depends linearly on the distance of the site i from the boundary as shown in the inset to Fig. 6. A corresponding bulk-to-boundary crossover between the

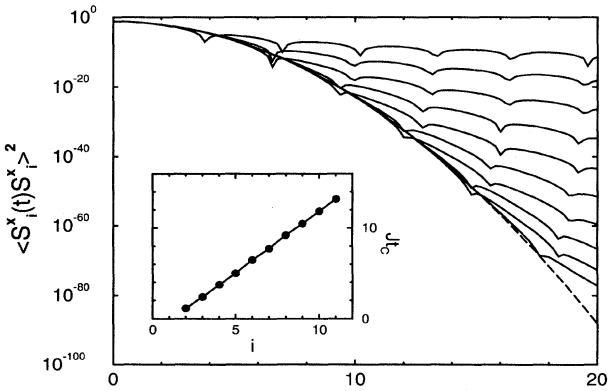

FIG. 6. Logarithmic plot of the square of the spin autocorrelation function $\langle S_i^x(t)S_i^x\rangle$ in the boundary regime of H_{XX} at $T = \infty$ for $i = 2, \ldots, 11$ (top to bottom). The dashed line represents the Gaussian (3.1) pertaining to the bulk limit ($i \to \infty$). The data for $i \leq 5$ are obtained from the exact expressions given in Ref. 4 and the data for $i > 5$ from an open chain with $N = 100$ spins. The inset shows the time Jt_c at which the relative deviation of $\langle S_i^x(t)S_i^x\rangle^2$ from the Gaussian first exceeds one percent.

power laws $t^{-1/2}$ and t^{-1} takes place in $\langle S_i^x(t)S_i^x\rangle$ at $T = 0$.

Now we keep the site fixed at $i = 2$ close to the boundary and vary the temperature. At high temperatures ($T/J \gg 1$) we can observe an infinite-to-finite-T crossover similar to the one portrayed in Fig. 1 for the bulk regime. But here in the boundary regime, it is a crossover between two power laws: $t^{-9/2}$ and $t^{-3/2}$. This crossover is illustrated in Fig. 7. The solid lines represent smoothed data at $2T/J = 10^3$ (top) and $2T/J = 10^5$ (bottom) in a log-log plot. It shows how the crossover is shifted to longer times as the temperature approaches infinity. A zero-to-nonzero-T crossover between the respective power laws t^{-1} and $t^{-3/2}$ can be observed at low temperatures ($T/J \ll 1$). This is illustrated in the inset to Fig. 7. Again the crossover is different from the corresponding (power-law-to-exponential) crossover in the bulk regime (Fig. 2).

The two types of crossover in $\langle S_i^x(t)S_i^x\rangle$ of the semi-infinite XX chain, which we have described separately, namely, the bulk-to-boundary crossover (Fig. 6) and the infinite-to-finite-T or zero-to-nonzero-T crossover (Fig. 7), may actually occur in one and the same data set. One case in point is demonstrated in Fig. 8. It shows a logarithmic plot of $|\langle S_i^x(t)S_i^x\rangle|^2$ at high temperatures ($T/J \gg 1$) for a site of the infinite chain (solid lines) and a site not too far from the end of a semi-infinite chain (dashed lines). The solid lines, which represent data already shown in Fig. 1, exhibit the familiar infinite-to-finite-T crossover pertaining to the bulk regime. The same crossover between decay laws (3.1) and (3.6) is also observable in the dashed lines, but here it is followed by the bulk-to-boundary crossover at finite T, i.e., between decay laws (3.6) and (4.3).

Note that in the lowest dashed curve, which corresponds to the highest temperature, the intermediate

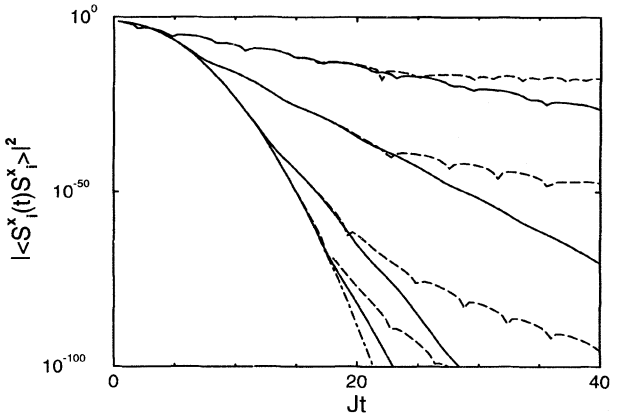

FIG. 8. Spin autocorrelation function $\langle S_i^x(t)S_i^x\rangle$ in the bulk regime and in the boundary regime of H_{XX} at high temperatures. Plotted is the logarithm of $|\langle S_i^x(t)S_i^x\rangle|^2$ evaluated at increments $Jdt = 0.4$ for site $i = 49$ (solid lines) and site $i = 11$ (dashed lines) in an open chain of $N = 100$ spins for $2T/J = 1$, 10, 10^3, and 10^5. The dot-dashed line represents the Gaussian decay law (3.1).

decay law has virtually disappeared. Here the two crossovers overlap. At still higher temperatures their order is reversed. The Gaussian decay law (3.1) crosses over (bulk to boundary) to the power law (4.1), which in turn crosses over (infinite to finite T) to the power law (4.3). Corresponding crossover combinations take place in the low-temperature regime.

ACKNOWLEDGMENTS

The work at URI was supported by the U. S. National Science Foundation, Grant No. DMR-93-12252 and by the NCSA Urbana Champaign. J.S. gratefully acknowledges the generous hospitality of the Department of Physics, University of Rhode Island, and the financial support of the Max Kade Foundation during the time when this work was begun. We thank L.L. Gonçalves for useful comments.

APPENDIX: DECAY LAWS IN THE BOUNDARY REGIME

The $t^{-3/2}$ decay law of the spin autocorrelation function $\langle S_i^x(t)S_i^x\rangle$ in the boundary regime at finite nonzero T can be recovered by the following analysis of the Pfaffian (2.8) and its elements. For $N \to \infty$ all nonvanishing expectation values (2.9) and (2.10) are equal to

$$f_{jl}(t) = \frac{4}{\pi}(-)^{j-l}\int_{-1}^{1} dx\, \sqrt{1-x^2}\, U_{j-1}(x)\, U_{l-1}(x) \times e^{iJxt}\, f(\beta Jx), \tag{A1}$$

where $f(x) = (e^x + 1)^{-1}$ is the Fermi function and $U_n(x)$ is a Chebyshev polynomial of the second kind. The long-time behavior of $f_{jl}(t)$ is determined by the singularities of its Fourier transform

$$\phi_{jl}(x) = \sqrt{1-x^2}\, U_{j-1}\,(x)U_{l-1}(x)\, f(\beta Jx)\, \Theta(1-x^2). \tag{A2}$$

At nonzero T the only singularities of (A2) are the square-root cusps $\sqrt{1-|x|}\,\Theta(1-|x|)$ at $x \to \pm 1$, which yield $f_{jl}(t) \sim e^{\pm iJt}t^{-3/2}$. At $T = 0$ an additional singularity in $\phi_{jl}(x)$ at $x = 0$ is generated by the discontinuity in the Fermi function, but it contributes only to leading order if both polynomials in (A2) are even, i.e., for odd j and l: $f_{jl}(t) \sim t^{-1}$.

Instead of the Pfaffian (2.8) we study the associated antisymmetric $(4i-2)\times(4i-2)$ matrix. Its determinant is equal to the square of (2.8) for $i = j$. That matrix naturally divides into four $(2i-1)\times(2i-1)$ blocks:

$$16\langle S_i^x(t)S_i^x\rangle^2 = \begin{vmatrix} \mathbf{M} & \mathbf{A} \\ \mathbf{A} & \mathbf{M}' \end{vmatrix}. \tag{A3}$$

The blocks $\mathbf{M}$ and $\mathbf{M}'$ contain only time-independent elements $f_{jl}(0)$ and the block $\mathbf{A}$ only time-dependent elements $f_{jl}(t)$. Block $\mathbf{M}$ turns out to have the following general structure:

$$\mathbf{M} = \begin{pmatrix}
0 & 0 & 0 & f_{12}(0) & 0 & 0 & 0 & f_{14}(0) & 0 & \cdots \\
0 & 0 & -f_{12}(0) & 0 & 0 & 0 & -f_{14}(0) & 0 & 0 & \cdots \\
0 & f_{12}(0) & 0 & 0 & 0 & f_{23}(0) & 0 & 0 & 0 & \cdots \\
-f_{12}(0) & 0 & 0 & 0 & -f_{23}(0) & 0 & 0 & 0 & -f_{25}(0) & \cdots \\
0 & 0 & 0 & f_{23}(0) & 0 & 0 & 0 & f_{34}(0) & 0 & \cdots \\
0 & 0 & -f_{23}(0) & 0 & 0 & 0 & -f_{34}(0) & 0 & 0 & \cdots \\
0 & f_{14}(0) & 0 & 0 & 0 & f_{34}(0) & 0 & 0 & 0 & \cdots \\
-f_{14}(0) & 0 & 0 & 0 & -f_{34}(0) & 0 & 0 & 0 & -f_{45}(0) & \cdots \\
0 & 0 & 0 & f_{25}(0) & 0 & 0 & 0 & f_{45}(0) & 0 & \cdots \\
\cdots & \cdots & \cdots & \cdots & \cdots & \cdots & \cdots & \cdots & \cdots & \cdots
\end{pmatrix}. \tag{A4}$$

Block $\mathbf{M}'$ has a similar distribution of nonzero elements. The leading long-time term in the expansion of (A3) is the one which contains the smallest possible number of time-dependent elements, i.e., the largest possible number of elements from $\mathbf{M}$ and $\mathbf{M}'$. Given the structure of $\mathbf{M}$, it is not possible to pick more than $2i-2$ elements from $\mathbf{M}$ in the expansion of (A3). The same holds true for $\mathbf{M}'$. Therefore, the leading term in (A3) contains exactly two time-dependent elements $f_{jl}(t)$ from $\mathbf{A}$, which explains the decay laws (4.2) and (4.3) at $T = 0$ and $0 < T < \infty$, respectively. At $T = \infty$ all elements of $\mathbf{M}$ and $\mathbf{M}'$ vanish, and the asymptotic long-time behavior is solely determined by block $\mathbf{A}$. This leads to the site-dependent decay law (4.1) as explained in Ref. 4.[29]

* Present address.
[1] J. M. R. Roldan, B. M. McCoy, and J. H. H. Perk, Physica A **136**, 255 (1986).
[2] M. Böhm and H. Leschke, J. Phys. A **25**, 1043 (1992).
[3] M. Böhm and H. Leschke, Physica A **199**, 116 (1993); **203** 328 (1994).
[4] J. Stolze, V. S. Viswanath, and G. Müller Z. Phys. B **89**, 45 (1992).
[5] M. Böhm, V. S. Viswanath, J. Stolze, and G. Müller, Phys. Rev. B **49**, 15669 (1994).
[6] Th. Niemeijer, Physica **36**, 377 (1967).
[7] S. Katsura, T. Horiguchi, and M. Suzuki, Physica **46**, 67 (1970).
[8] B. M. McCoy, E. Barouch, and D. B. Abraham, Phys. Rev. A **4** 2331 (1971).
[9] H. G. Vaidya and C. A. Tracy, Physica **92A**, 1 (1978).
[10] B. M. McCoy, J. H. H. Perk, and R. E. Shrock, Nucl. Phys. **B220** [FS8], 35 (1983); **B220** [FS8], 269 (1983).
[11] G. Müller and R. E. Shrock, Phys. Rev. B **29**, 288 (1984).
[12] A. Sur, D. Jasnow, and I. J. Lowe, Phys. Rev. B **12**, 3845 (1975).
[13] U. Brandt and K. Jacoby, Z. Phy. B **25**, 181 (1976).
[14] H. W. Capel and J. H. H. Perk, Physica **87A**, 211 (1977).
[15] A. R. Its, A. G. Izergin, V. E. Korepin, and N. A. Slavnov, Phys. Rev. Lett. **70**, 1704 (1993).
[16] E. Lieb, T. Schultz, and D. Mattis, Ann. Phys. (N.Y.) **16**, 407 (1961).
[17] S. Katsura, Phys. Rev. **127**, 1508 (1962).
[18] S. Sen, S. D. Mahanti, and Z.-X. Cai, Phys. Rev. B **43**, 10990 (1991).
[19] W. Pesch and H. J. Mikeska, Z. Phys. B **30**, 177 (1978).
[20] One successful early application of this method at $T = 0$ was reported in Ref. 19.
[21] L. L. Gonçalves and H. B. Cruz, J. Magn. Magn. Mater. **15-18**, 1067 (1980).
[22] References on the properties of Pfaffians and on their use for the calculation of dynamic correlations in XX chains can be found, for example, in Appendix A of Ref. 4.
[23] H. B. Cruz and L. L. Gonçalves, J. Phys. C **14**, 2785 (1981).
[24] An earlier attempt by M. Mohan [Phys. Rev. B **21**, 1264 (1980); **23**, 433 (1981)] to determine the decay law of $\langle S_i^x(t)S_i^x\rangle$ in the vicinity of the high-temperature limit produced the result $\sim \exp[-J^2t^2/4\{1-4/\ln(Jt/2)\}]$, obtained from a high-temperature series expansion. This modified Gaussian, which was asserted to hold for $Jt > \ln(2T/J)$, does, however, not show the slightest similarity with any of the results in Fig. 1; nor is it consistent with the asymptotic result (3.6).
[25] A. Nöppert and J. Stolze (unpublished).
[26] B. M. McCoy, Phys. Rev. **173**, 531 (1968).
[27] E. Barouch and B. M. McCoy, Phys. Rev. A **3**, 786 (1971).
[28] T. Tonegawa, Solid State Commun. **40**, 983 (1981).
[29] The t^{-2} and t^{-3} decay laws of the spin pair correlation function $\langle S_i^z(t)S_j^z\rangle$ in the boundary regime can be explained by observing that $4\langle S_i^z(t)S_j^z\rangle = (-)^{i-j}[f_{ij}(t)]^2$.